

# Advantages of flexible musculoskeletal robot structure in sensory acquisition

Shuhei Ikemoto<sup>1</sup>, Yoichi Nishigori<sup>2</sup>, and Koh Hosoda<sup>1</sup>

<sup>1</sup> Graduate School of Information Science and Technology, Osaka University, Osaka, Japan

<sup>2</sup> Graduate School of Engineering, Osaka University, Osaka, Japan

(Tel: 81-06-6879-7739, Fax: 81-06-6879-7750)

(ikemoto@ist.osaka-u.ac.jp)

**Abstract:** Morphological computation is the concept for which a well-designed hardware can bear part of the computational cost required for robot's control and perception. So far, many musculoskeletal robots have been developed by taking inspiration from human's one and shown superior motion performances. The use of pneumatic artificial muscles (PAMs) has been the key to realize these high performance. Additionally, PAMs have the possibility of being used as sensors for environmental information because they are flexible and backdrivable. In this research, we focus on clarifying how PAMs can contribute to morphological computation of robots driven by these actuators. In particular, we propose an analysis method based on transfer entropy and apply this method to the experimental data acquired by a musculoskeletal robot that opens a door.

**Keywords:** musculoskeletal robot, pneumatic artificial muscle, transfer entropy

## 1 INTRODUCTION

Creating a robot inspired from biological systems has been an attractive approach for many researchers in robotics. Especially, human's musculoskeletal system has been often focused because it was optimized to realize intelligent motions during the whole evolutionary history of humans. So far, many musculoskeletal robots that exploit information processing provided by well-designed musculoskeletal structures were proposed. This information processing is called morphological computation and it is one of the key words that symbolize the field of the artificial intelligence paying attention to the embodiment[1].

Artificial pneumatic muscles (PAMs) have been one of most suitable actuators to develop musculoskeletal robots. Thanks to useful features proper of PAMs such as flexibility, backdrivability and high power-to-weight ratio, musculoskeletal robots driven by PAMs have successfully shown superior motion performances[2][3]. Additionally, PAM's state have sometimes been used as a sensor[4] that provides information on the external world and on the state of the robot. This information can be interpreted as proprioceptive information of the musculoskeletal robot and we think that this point is notably important to understand morphological computation in robot's perception. However, in previous researches, the PAM (among the robot's numerous PAMs) that contains important information on the external world was required to be known beforehand and the air-flow to/from such PAM had to be set to zero during the sensing process.

In this research, we focus on morphological computation of musculoskeletal robot's perception using flexibility of PAMs. In particular, in this paper, we aim to show that acquiring environmental information is possible even while the

PAM is being driven. Additionally, we don't specify which PAM notably contains environmental information in advance and figure out which PAM is important from the data of all PAMs available in the robot. To this end, we use a musculoskeletal robot arm able to easily open a door by exploiting the morphological computation provided by the flexibility of PAMs. Additionally, we propose an analysis method based on transfer entropy to investigate whether or not PAMs driving the robot arm can contain environmental information. Finally, we apply the proposed method to the data taken in a door-opening task and discuss the analysis results.

## 2 MUSCULOSKELETAL ROBOT ARM

In this research, we use a musculoskeletal robot arm developed in our research group. This robot arm is driven by PAMs and has several sensors to control and observe the states.

### 2.1 Hardware design

Fig.1 shows the developed musculoskeletal robot and the configuration of its degrees of freedom. This robot has 7 degrees of freedom(DOF) in its skeletal structure and the configuration is schematically similar to the human's one. For example, the robot arm employs a radioulnar joint and an ellipsoidal joint in the forearm and the wrist, respectively[5]. Fig.2 shows the layout of the PAMs in the robot. The robot is equipped with 17 groups of PAMs for driving its skeletal structure. Because the PAMs have flexibility and backdrivability, the arm can change the posture accordingly to exerting external force. The layout of the PAMs presents similarity with human muscles as well. For example, most of PAMs are configured in the form of antagonistic pairs and there are not only monoarticular muscles but also biarticu-

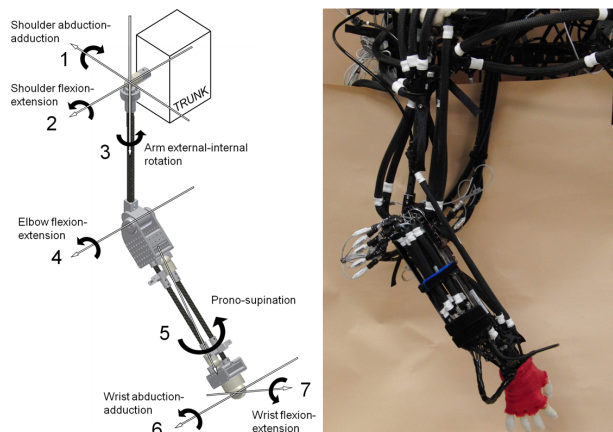


Fig. 1. The 7-DOF musculoskeletal robot arm. The structure is schematically similar to the one of humans and it is driven by PAMs.

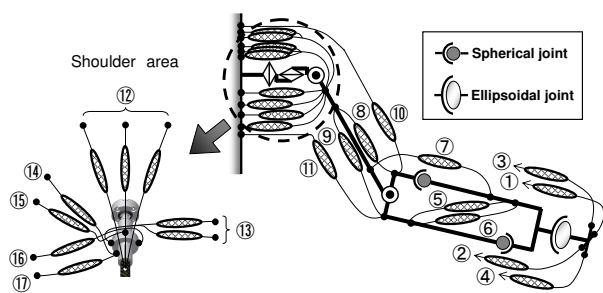


Fig. 2. PAMs layout of the developed pneumatic robot arm. There are 17 different groups of PAMs in the robot arm. Muscles having the same muscle ID are controlled as if they were a single muscle

lar muscles[5]. Additionally, the robot mounts a robot hand driven by PAMs at the end of the arm[6].

In order to investigate whether or not acquiring environmental information from PAMs is possible even if PAMs are being driven, the robot arm was equipped with several kinds of sensors. Since analytical models of PAM's statics have three variables, namely pressure, tension and length, it is obvious that at least two of three variables have to be measured to know the static state[7] of the PAM. In the musculoskeletal robot arm, pressure and tension sensors are available for all PAMs and all PAMs except the robot hand, respectively.

## 2.2 Control system

So far, many researches have focused on controlling PAMs and the statics was modeled accurately[7]. However, since the analytical models are very complex, it is very difficult to fully consider these models to generate motions of musculoskeletal robots driven by PAMs. Therefore, simple pressure feedback control has been often used[8][9]. In this

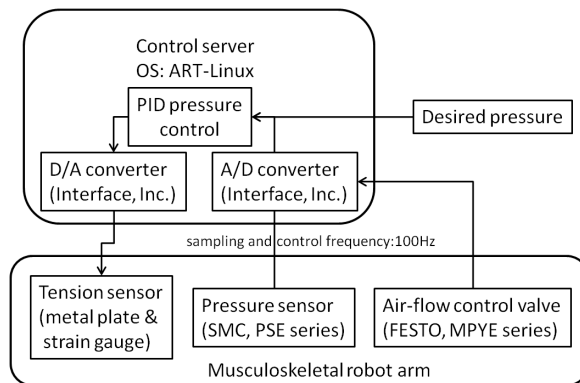


Fig. 3. Control system of the developed musculoskeletal robot.

research, we also adopt a pressure feedback system based on PID control.

Fig.3 shows the control system of the robot. Note that all the sensor information and control signal can be recorded during an experiment. For the control server, ART-Linux<sup>1</sup> is employed to ensure realtime data sampling and control. Because the control system shown in Fig.3 needs only the pressure information from all PAMs, the tension sensor information is recorded only for analysis purposes. Actually, the tension sensor information is very important for the analysis because the robot can assume different postures with the same pressures depending on the tensions.

## 3 MOTION ANALYSIS OF MUSCULOSKELETAL ROBOT

When a musculoskeletal robot is controlled by a time-series of desired pressures, the obtained sensor data has a lot of information about the desired pressures. Therefore, it is required to analyze the differences caused by changes of external force exerted by physical contact and dynamics of the robot. In this research, we focus on transfer entropy to extract these differences.

### 3.1 Transfer entropy

Transfer entropy is a measure which can quantify nonlinear relationships among stochastically generated time-series of data and a stochastic variable. Intuitively speaking, transfer entropy quantifies dynamic information flow, by measuring how large the influence from a stochastic variable to a time-series of data is. Additionally, transfer entropy can quantify the information flow correctly even in the cases where the two stochastic variables are influenced by another stochastic variables. Recently, transfer entropy has been exploited in

<sup>1</sup>A realtime operating system based on Linux developed by National Institute of Advanced Industrial Science and Technology in Japan: <http://www.dh.aist.go.jp/en/research/humanoid/ART-Linux/>

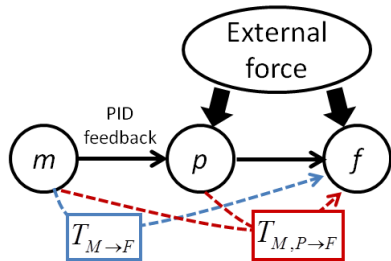


Fig. 4. The schematic relationship among  $M$ ,  $P$ ,  $F$  and the external force .

the robotics field to find out causalities among robot sensor data[10].

Transfer entropy between two discrete stochastic variables  $I$  and  $J$  can be defined as:

$$T_{J \rightarrow I} = \sum_{i_{n+1}, i_n, j_n} P(i_{n+1}, i_n, j_n) \log \frac{P(i_{n+1}|i_n, j_n)}{P(i_{n+1}|i_n)} \quad (1)$$

Where  $n$  is a discrete time. This indicates that the transfer entropy is similar to Kullback-Leibler divergence between a probability distribution assuming  $I$  has Markov property and a probability distribution assuming  $I$  is a subject to  $J$ .

### 3.2 Analysis method

Considering the ideal condition of pressure feedback control, in which the desired pressure  $M$  is exactly corresponding to the actual pressure  $P$ , the subsidiarity of  $F$  to  $M$  or  $P$  can be expressed by using transfer entropy written as following:

$$\begin{aligned} T_{M \rightarrow F} &= \sum_{f_{t+1}, f_t, m_t} P(f_{t+1}, f_t, m_t) \log \frac{P(f_{t+1}|f_t, m_t)}{P(f_{t+1}|f_t)} \\ &= T_{P \rightarrow F} \\ &= T_{M, P \rightarrow F} \end{aligned} \quad (2)$$

As explained in the beginning of this section, the aim of the analysis is investigating the difference caused by changes of external force exerted by physical contact and dynamics of the robot. To this end, we evaluate the difference by using the ideal condition Eq.2 as the baseline.

In order to consider the qualitative meaning of  $T_{M \rightarrow F}$  and  $T_{M, P \rightarrow F}$  in the actual condition, we show the relationship among  $M$ ,  $P$ ,  $F$  and the external force schematically in Fig.4. In the actual condition, the error on the pressure feedback control has to be caused by external force derived from physical contact with the environment and by the dynamics of the robot. As a result,  $T_{M \rightarrow F}$  and  $T_{M, P \rightarrow F}$  have to be different. Considering how  $T_{M \rightarrow F}$  and  $T_{M, P \rightarrow F}$  change compared to the ideal condition,  $T_{M, P \rightarrow F}$  is larger than  $T_{M \rightarrow F}$  in most cases since the  $M, P$  will has larger information on the external force than the  $M$  alone.

In this paper, we evaluate the difference  $T_{M, P \rightarrow F}^C = T_{M, P \rightarrow F} - T_{M \rightarrow F}$  as a measure on how the dynamics of the robot and physical contacts with the environment influence the PAM's states. This measure can be interpreted as the fact that it is possible to subtract the effect of the  $M$  because both  $T_{M \rightarrow F}$  and  $T_{M, P \rightarrow F}$  contain the information flow from the  $M$  to the  $F$ .

The  $T_{M, P \rightarrow F}$  can be written as following:

$$T_{M, P \rightarrow F} = \sum_{f_{t+1}, f_t, m_t, p_t} P(f_{t+1}, f_t, m_t, p_t) \log \frac{P(f_{t+1}|f_t, m_t, p_t)}{P(f_{t+1}|f_t)} \quad (3)$$

Subtracting  $T_{M \rightarrow F}$  from Eq.3,  $T_{M, P \rightarrow F}^C$  can be written as following:

$$\begin{aligned} T_{M, P \rightarrow F}^C &= T_{M, P \rightarrow F} - T_{M \rightarrow F} \\ &= \sum_{f_{t+1}, f_t, m_t, p_t} P(f_{t+1}, f_t, m_t, p_t) \log \frac{P(f_{t+1}|f_t, m_t, p_t)}{P(f_{t+1}|f_t, m_t)} \end{aligned} \quad (4)$$

As explained above, this measure  $T_{M, P \rightarrow F}^C$  should indicate how external force influences the PAMs. Note that  $T_{M, P \rightarrow F}^C$  does not have theoretical validity although similar method can be found in related research[10]. Additionally, we note that  $T_{M, P \rightarrow F}^C$  is applied individually for all PAMs in the robot arm without specifying which PAM should be focused.

## 4 EXPERIMENT

In this research, we focus on a door-opening task as an example of task in which both exerting and changing external force are present. At first, we will explain about the door-opening task used in the experiment, which can be attained by using the morphological computation of the musculoskeletal robot shown in Fig.1. In the following, we apply the proposed analysis method based on transfer entropy to the data obtained in the door-opening task.

### 4.1 Door-opening task

The door-opening task is a task in which a robot arm reaches a doorknob, grasps it and opens the door. For the musculoskeletal robot shown in Fig.1, the door-opening task is one of most suitable task to exploit its morphological computation because of the flexibility and backdrivability offered by the PAMs.

Fig.5 shows the sequential snapshots of the robot's motion during door-opening task. The sequence of desired pressures was designed through a trial-and-error process. However, the process is not very complex because it is possible to safely come in contact to the doorknob and move according to the physical constraints imposed by the doorknob easily due to the flexibility of the PAMs. For instance, the rotating and



Fig. 5. The execution of the door-opening task. The developed musculoskeletal robot arm can adaptively grasp and rotate the door knob, and open the door by exploiting its morphological computation.

the opening can be accomplished by inaccurate control because the physical constraints of the door hardly limits the robot motions and guides them to the few available motions when the robot hand is fixed on the doorknob. Since the door-opening consists in a reaching, rotating and opening phase as shown in Fig.5, it is a good example in which the differences previously explained are caused by changes of external force exerted by physical contacts and by the dynamics of the robot.

In addition to the three phases in the door-opening task, we add following three conditions of the task:

1. normal condition (successful trial)
2. locked condition (the door does not open)
3. uncontact condition (failure in reaching the doorknob)

In this paper, we analyze the data obtained in these three conditions. In particular, we investigate how different the  $T_{M,P \rightarrow F}^C$  are in the three phase of the door-opening task and in the three different conditions.

#### 4.2 Result

For the analysis, 10 trials data were collected for each three conditions. In each trials, the robot arm starts reaching in 0.9 seconds from the beginning of the trial, grasps and rotates the doorknob at 1.0 seconds and pulls it for 3.0 second after the rotation. In comparison with the first condition, the second condition will differ in the second phase and the third condition will be differ after touching the doorknob. It can be assumed that these differences among three conditions and three phases will be observed by  $T_{M,P \rightarrow F}^C$ .

Fig.6 shows the average of  $T_{M,P \rightarrow F}^C$  value in ten trials of each conditions. The error bar indicates the standard deviation. The left of Fig.6 shows the  $T_{M,P \rightarrow F}^C$  value for each

PAMs in the reaching phase. In the reaching phase, there is no difference among the three conditions except that for the third condition the contact with the doorknob does not occur at the end of the phase. Small differences can be observed in muscle 1, 2, 3 and 4 which drive the wrist of the robot arm as shown in Fig.2. Therefore, the analysis results are reasonable for the reaching phase.

The middle of Fig.6 shows the result for the rotating phase. In this phase, the third condition is very different from the others because it is not physically constrained by the door. From the result, it can be observed that there is a large difference in muscles 6, 7 and 16 between the third condition and the others. Considering the physical meaning of why these  $T_{M,P \rightarrow F}^C$  values are larger in the third condition, we note that these muscles will get a large reaction force from the know when this is grasped and rotated, if the robot hand is actually fixed on the doorknob. In other words, in the first and the second conditions, the robot motions have to obey the physical constraints imposed by the door. As a consequence, we can assume that the  $T_{M,P \rightarrow F}^C$  value captured the environmental information reflected in muscle 6, 7 and 16 for the third condition.

The right of Fig.6 shows the results for the opening phase. In this phase, the second condition provides large resistance in moving the arm because the door is locked and does not open. Therefore, the  $T_{M,P \rightarrow F}^C$  value will be increased in the second condition because the change of the pressure will be more directly easily reflected in the change of the tension. In the right of Fig.6, it can be seen that the  $T_{M,P \rightarrow F}^C$  values for almost muscles in the second condition are larger than the same values in the first condition. In the third condition, the  $T_{M,P \rightarrow F}^C$  values of some muscles, such as muscle 8 and 10, are larger than the value for the same quantities in the

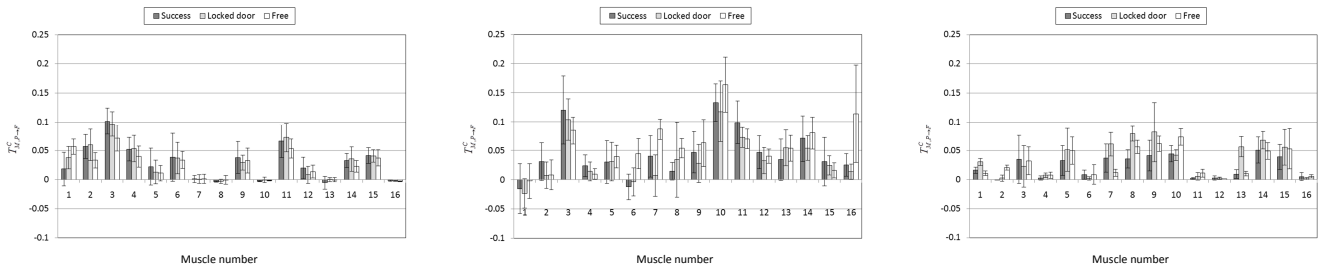


Fig. 6. The  $T_{M,P \rightarrow F}^C$  in three conditions and three phases.

first condition. This indicates that physical constraints sometimes reduce the resistance of gravity because muscle 8 and 10 mainly bear the weight of the arm in this posture.

Through this experiment, it is qualitatively confirmed that PAMs driving the robot arm can be exploited to extract environmental information such as external force derived from physical contacts with the environment and from the dynamics of the robot. However, this is still a preliminary result that needs to be validated in order to confirm the main concept of this research. Future works will deal with more extensive experiments to validate our hypothesis, supported by the current preliminary results.

## 5 DISCUSSION AND CONCLUSION

In this research, we focused on morphological computation in a robot's perception that exploits the PAM's features. In particular, we focused on the possibility of PAMs to contribute to morphological computation of robots driven by these actuators. To this end, we proposed an analysis method based on transfer entropy and applied this method to the data taken from an experiment in which a musculoskeletal robot opens a door. As a consequence, it was qualitatively confirmed that the PAMs actuating the musculoskeletal robot arm can be used to obtain environmental information such as physical contacts and the dynamics of the robot even when these are actively actuated. Additionally, it was verified that the analysis method can be applied without specifying beforehand which PAMs should be focused.

The result in this paper can be used for finding out which PAM are useful to learn or improve the musculoskeletal robot's motions. In fact, one of biggest problems to control complex musculoskeletal robots driven by PAMs is the high dimensionality of the state and the motor command spaces derived from the structural complexity. The experiment showed the possibility that few PAMs could be able to generate the robot's motion appropriately and could be used as sensors to extract information on the surrounding environment.

However, the result obtained in this research is still very preliminary. Therefore, it will be necessary to investigate

both of the robot's structure and the analysis method for clarifying morphological computation offered by musculoskeletal structures.

## REFERENCES

- [1] R.eifer and J.Bongard. *how the body shapes the way we think. a new view of intelligence*. MIT Press, 2006.
- [2] Ryuma Niiyama, Satoshi Nishikawa, and Yasuo Kuniyoshi. Athlete robot with applied human muscle activation patterns for bipedal running. In *Proc. IEEE-RAS Int. Conf. on Humanoid Robots (Humanoids 2010)*, pages 498–503. Nashville, Tennessee USA, Dec. 2010.
- [3] Ryuma Niiyama, Akihiko Nagakubo, and Yasuo Kuniyoshi. Mowgli: A bipedal jumping and landing robot with an artificial musculoskeletal system. In *Proc. IEEE Int. Conf. on Robotics and Automation (ICRA 2007)*, pages 2546–2551 (ThC5.2), Roma, Italy, April 2007.
- [4] K. Hosoda, H. Takayama, and T. Takuma. Bouncing monopod with bio-mimetic muscular-skeleton system. In *Intelligent Robots and Systems, 2008. IROS 2008. IEEE/RSJ International Conference on*, pages 3083–3088. IEEE, 2008.
- [5] D.A. Neumann and D.L. Wong. *Kinesiology of the musculoskeletal system: foundations for physical rehabilitation*. Mosby St Louis, MO, 2002.
- [6] Alejandro Hernandez Arieta and Hiroshi Yokoi. Integration of a multi-d.o.f. individual adaptable with tactile feedback for an emg prosthetic system. *Intelligent Autonomous Systems*, 8:pp.1013–1021, 2004.
- [7] C.P. Chou and B. Hannaford. Measurement and modeling of McKibben pneumatic artificial muscles. *IEEE Transactions on Robotics and Automation*, 12(1):90–102, 1996.
- [8] B.Tondu, S.Ippolito, J.Guiochet, and A.Daidie. A seven-degrees-of-freedom robot-arm driven by pneumatic artificial muscle for humanoid robots. *The International Journal of Robotics Research*, 24(4):257–274, 2005.
- [9] N.Nakamura, M.Sekiguchi, K.Kawashima, T.Fujita, and T.Kagawa. Developing a robot arm using pneumatic artificial rubber muscles. *Power Transmission and Motion Control*, 2002.
- [10] Y.Yoshikawa H.Sumioaka and M.Asada. Learning of joint attention from detecting causality based on transfer entropy. *Journal of Robotics and Mechatronics*, 20(3):378–385, 2009.